Int. J. Electrochem. Sci., 16 **(2021)** Article ID: 21098, doi: 10.20964/2021.09.23

International Journal of
ELECTROCHEMICAL
SCIENCE
www.electrochemsci.org

Mini review

Electrochemical Methods for the Detection of Poly(ADP-ribose) Polymerase-1

Ting Sun[1,2], *Yanying Li*[1] *and Feng Zhao*[1,*]

[1] School of Chemistry and Materials Science, Guizhou Education University, Guizhou, 550000, People's Republic of China
[2] College of Chemistry and Chemical Engineering, Anyang Normal University, Anyang, Henan 455000, People's Republic of China
[*]E-mail: fygu2010@163.com

Received: 15 May 2021 / *Accepted:* 30 June 2021 / *Published:* 10 August 2021

Poly(ADP-ribose) polymerase-1 (PARP-1) plays an important role in DNA repair and apoptosis. The enzyme has been regarded as the biomarker for many diseases including cancer. Therefore, simple, sensitive and rapid detection of PARP-1 is of great significance for early diagnosis and medical treatment. Electrochemistry-based biosensors have attracted much attention due to their low cost, simple operation, rapid response and high sensitivity. In this work, we summarized the electrochemical strategies for determining PARP-1 activity and screening the potential inhibitors.

Keywords: Poly(ADP-ribose) polymerase-1; electrochemistry; phenylboronic acid; electrostatic interaction

1. INTRODUCTION

Poly(ADP-ribose) polymerase-1 (PARP-1) is a multifunctional enzyme for protein modification, which exists in eukaryotic cells and plays an important role in DNA repair and apoptosis [1-3]. The enzyme is believed to be the biomarker and target for diagnosis and treatment of lung, breast, ovarian and other cancers [4-7]. Therefore, simple, sensitive and rapid detection of PARP-1 is of great significance for early diagnosis of cancers and discovery of novel anti-cancer drugs.

PARP-1 could be activated when interacting with the damaged DNA. The activated PARP-1 can cleave β-nicotinamide adenine dinucleotide (NAD^+) to produce adenosine diphosphate (ADP) ribose and nicotinamide. During the enzymatic reaction, ADP-ribose is covalently linked to the receptor proteins such as histone, transcription factor and PARP-1 itself, thus achieving the ribosylation of proteins. The numerous ADP-ribose units can be polymerized into linear or branched

poly(ADP-ribose) (PAR) polymers, in which PAR-ribose units less than 200 in length are located in the linear region of the polymer and those with a length of 20-50 are located in the branching domain (Fig. 1) [8]. The resulting polymers change the size and charge of receptor proteins, thereby initiating the regulation and repair of DNA lesion. NAD^+ or its analogue is commonly used as the substrate for PARP-1 assay and inhibitor screening. High performance liquid chromatography and immune array often require anti-PAR antibody to detect the formation of PAR polymers [9, 10]. The methods are time-consuming and expensive and/or need complex derivatization processes. Recently, colorimetry, fluorescence, electrochemistry, photoelectrochemistry, QCM and ATR-FTIR attenuated total reflection spectrometry have been widely reported for the assays of PARP-1 [11-23]. For instance, NAD^+ can be adsorbed on the nanoparticle surface to prevent the salt-induced aggregation of AuNPs. PARylation led to the cleavage of NAD^+ molecules, thus promoting the salt-induced aggregation and color change of AuNPs and allowing for the detection of PARP-1 [18]. In addition, the dispersed hemin-graphene nanocomposites can catalyze the chromogenic reaction of tetramethylbenzidine by hydrogen peroxide. The salt (NaCl) can trigger the aggregation of hemin-graphene nanocomposites, thus depressing their peroxidase-like activity. The resulting PAR polymers can be adsorbed on the surface of hemin-graphene nanocomposites to protect their aggregation and facilitate colorimetric detection of PARP-1 [15]. The fluorescence of cationic conjugated polymer can be quenched by MnO_2 nanosheets; Wu and co-workers found that the PAR polymers can be adsorbed on the surface of positively charged MnO_2 nanosheets, thus leading to the release and follow-up fluorescent recovery of PFP [13]. Recently, Wei's group reported a spectral-resolved single-particle biosensor for PARP-1 assay using dark-field microscopy (DFM) (Fig. 2). AuNPs with a size of 50 nm (Au_{50}) were modified with DNA duplexes as the scattering probes. The produced Au_{50}-dsDNA@PAR allowed for the adsorption of the positively charged AuNPs (8 nm). The resulting Au_{50}-dsDNA@PAR@Au8 exhibited a remarkable red shift, which is accompanied by the color change. Among these techniques, electrochemical biosensors have attracted much attention due to their low cost, simple operation, rapid response and high sensitivity [24]. In this work, we summarized the electrochemical strategies for determining PARP-1 activity and screening the potential inhibitors.

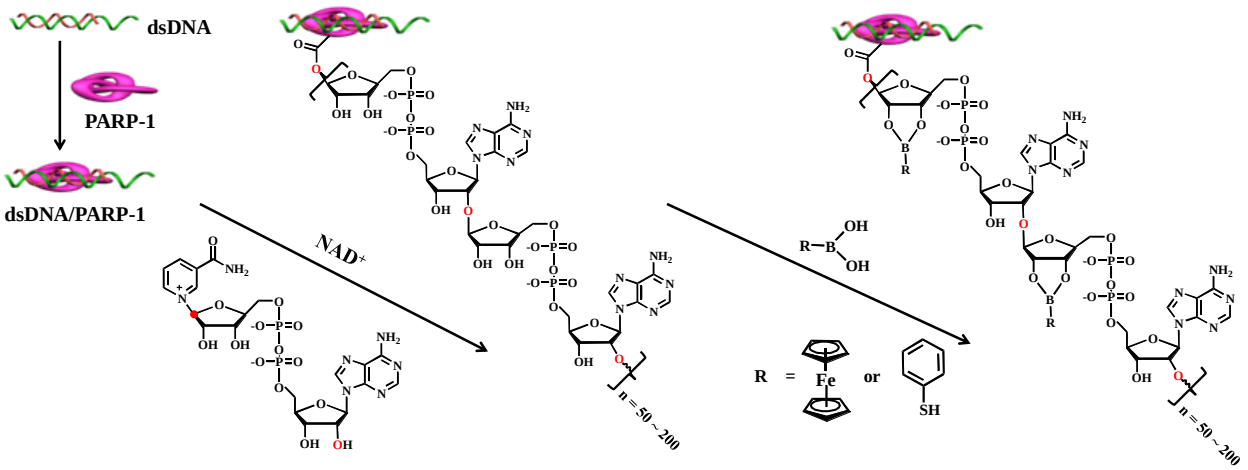

Figure 1. Schematic illustration of the catalyzed reaction by PARP-1 and the interaction between boronic acid derivates and ADP-ribose units. Reprinted with permission from reference [8]. Copyright 2021 Elsevier.

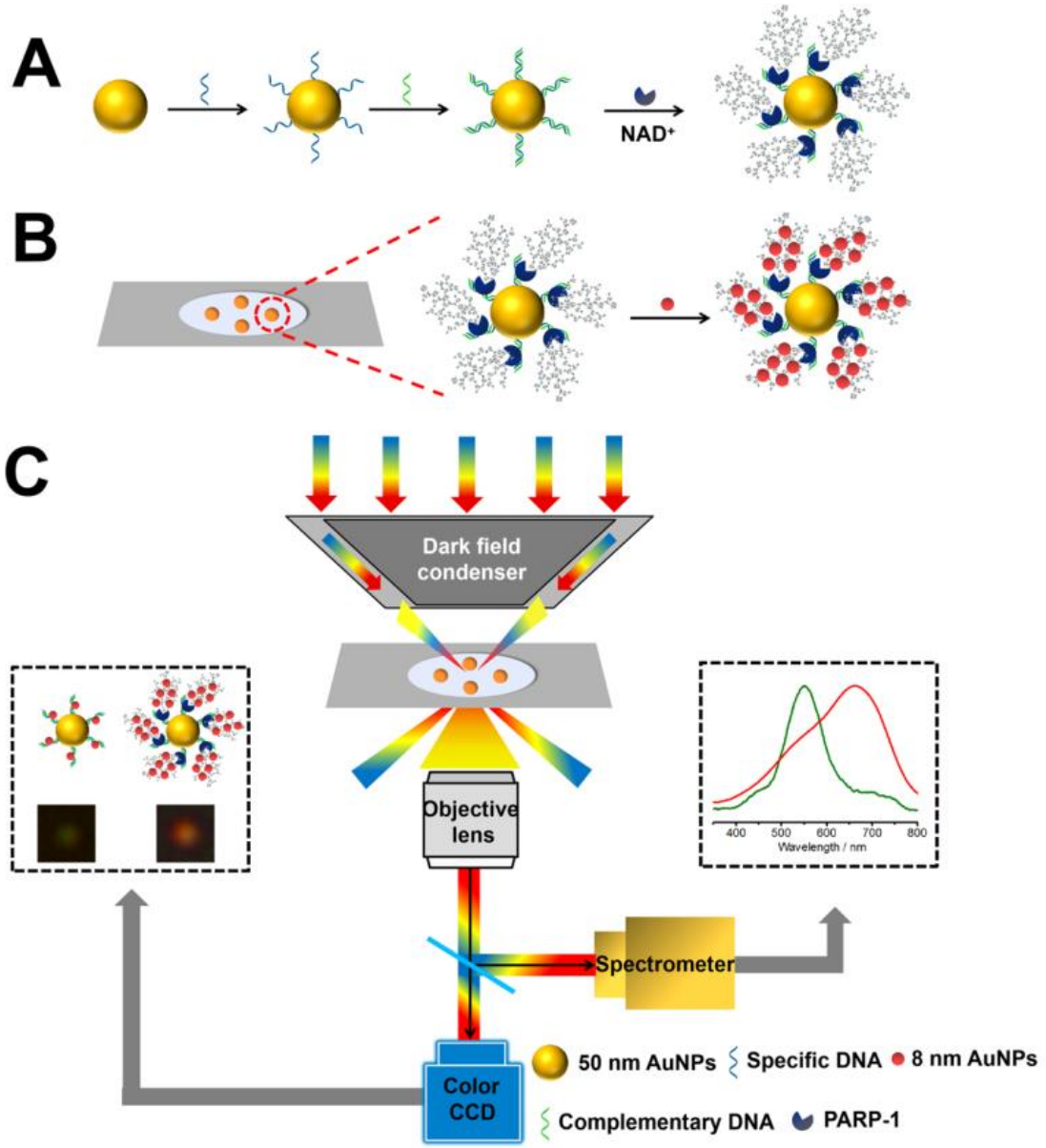

Figure 2. Schematic diagram for SPD and imaging of PARP-1 under DFM; (A) synthesis process of Au_{50}-dsDNA@PAR; (B) assembly of Au_{50}-dsDNA@PAR and Au_8; (C) diagram of single-particle assay for PARP-1 activity by using DFM. Reprinted with permission from reference [19]. Copyright 2020 American Chemical Society.

2. ELETROCHEMICAL METHODS FOR PARP-1 DETECTION

Both the linear and branched PAR polymers contain large numbers of negatively charged phosphate groups, which facilitated the electrostatic interaction on the sensing interface or with electroactive molecules. For this view, many electrochemical strategies have been developed for PARP-1 detection. For instance, Xu and co-workers designed an electrochemical biosensor for the assay of PARP-1 and evaluating the inhibition efficiency based on the enzyme-initiated self-

polymerization glycosylation reaction [25]. As shown in Fig. 3, the DNA probe modified on electrode surface with the G-quadruplex structure can bind and activate PARP-1, thus catalyzing the production of negatively charged PAR polymers from NAD^+. The resulting PAR polymers facilitated the accumulation of positively charged hexaammineruthenium(III) chloride (RuHex) to produce a strong electrochemical signal. The linear range for PARP-1 detection was 0.01 ~ 1 U/mL with a detection limit of 3 mU/mL (Table 1). After that, they developed a label-free electrochemical biosensor for PARP-1 detection based on the electrostatic interaction between negatively charged PAR polymer and positively charged aminated mesoporous silica films (NH_2-MSFs) [26]. The PAR product adsorbed on the surface of NH_2-MSFs prevented $[Fe(CN)_6]^{3-/4-}$ from approaching to the ITO electrode. As a result, the electrochemical signal was weakened. The linear range for PARP-1 detection is 0.01 ~ 1.2 U/mL. The detection limit was found to be 5 mU/mL. The method can be applied to evaluate PARP-1 inhibitor and determine PARP-1 in serums and tumor cell lysates. Liu et al. reported that the double-stranded DNA (dsDNA) can bind to PARP-1 and catalyze the formation of PAR polymer [27]. The activity of PARP-1 can be determined by electrostatic deposition of positively charged polyaniline on its surface. By measuring the reduction peak of deposited polyaniline, PARP-1 has been determined in the linear range of 0.005 ~ 1 U/mL with a detection limit of 2 mU/mL.

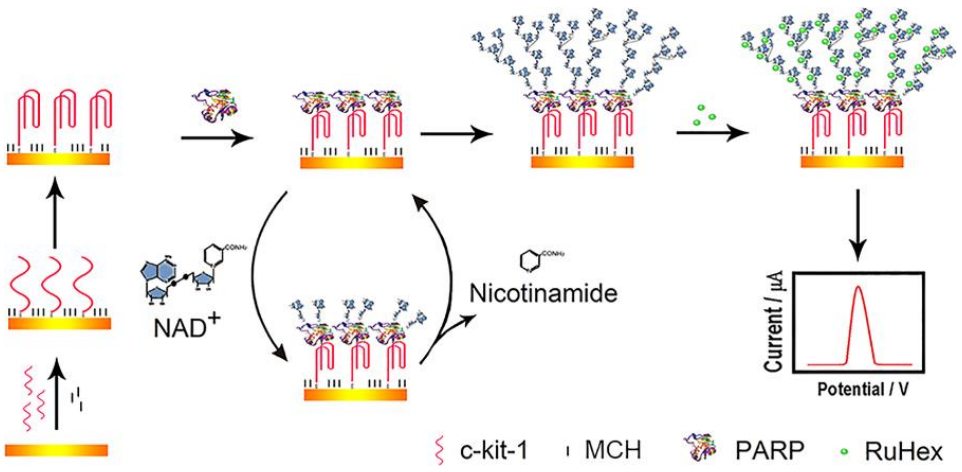

Figure 3. Schematic illustration of a stable and reusable electrochemical biosensor for poly(ADP-ribose) polymerase and its inhibitor based on enzyme-initiated auto-PARylation. Reprinted with permission from reference [25]. Copyright 2016 American Chemical Society.

The organic reaction is not only affected by its own structure, activity and reaction conditions, but also closely related to the external environment such as the host-guest effect. For this consideration, Zhou et al. reported an electrochemical method for PARP-1 assay through the host-guest reaction [28]. In this work, β-cyclodextrin was immobilized onto the electrode surface for the attachment of trans azobenzene-labeled dsDNA. PARP-1 could catalyze the hydrolysis of NAD^+ to synthesize PAR polymers. Then, MoO_4^{2-} was captured by the surface-rich PO_4^{3-} groups, thus generating a strong electrochemical signal. This strategy shows no non-specific adsorption and at the same time improved the detection sensitivity. After UV irradiation, azobenzene changed from trans to cis configuration and then released from the electrode. The linear range for PARP-1 analysis was 0.01 ~ 1 U/mL, and the detection limit was 8 mU/mL. Wang and co-workers proposed a specific and

efficient electrochemical method for PARP-1 assay using different peptide templates and copper nanoparticles (CuNPs) arrays [29]. Peptide containing guanidine groups was used as the reducing agent for the preparation of CuNPs. Moreover, the guanidine groups on the surface of CuNPs bound with phosphate groups of PAR polymers. PARP-1 has been successfully determined by measuring the oxidation signal of CuNPs.

Table 1. Analytical performances of various methods for PARP-1 detection.

Method	Signal reportor	Linear range	Detection limit	Ref.
Colorimetry	NAD-protected gold nanoparticles	0.43-1.74 nM	0.32 nM	[18]
Colorimetry	CTAB-coated GNRs	0.05–1.0 U	0.006 U	[17]
Colorimetry	hemin-graphene nanocomposites	0.05–1.0 U	0.003 U	[15]
Fluorescence	CCP and scGFP	1-45 nM	1 nM	[21]
Fluorescence	CCP and MnO_2 nanosheets	0.024-1.2 nM	0.003 nM	[13]
Fluorescence	TOTO-1	0.02–1.5 U	0.02 U	[14]
PEC	CCP	0.01-2 U	0.007 U	[30]
QCM	CTAB-coated GNRs	0.06-1.2 nM	0.04 nM	[20]
Electrochemistry	FcBA	0.1-50 U	0.1 U	[8]
Electrochemistry	Positively charged $[Ru(NH_3)_6]^{3+}$	0.01-1 U	0.003 U	[25]
Electrochemistry	Polyaniline deposition	0.005-1.0 U	0.002 U	[27]
Electrochemistry	Artificial nanochannels	0.05-1.5 U	0.006 U	[22]
Electrochemistry	Mesoporous silica films	0.01-1.2 U	0.005 U	[26]
Electrochemistry	$PMo_{12}O_{40}^{3-}$	0.01-1.0 U	0.008 U	[28]

The PAR polymers contain both numerous phosphate groups and cis-diol moieties in the ribose units. Phenylboronic acid and its derivatives can form five or six membered borate ester compounds with cis-diol derivatives. Such an interaction is often used for the separation and purification of diol-containing biomolecules [31-35]. We found that ferrocenylboronic acid (FcBA) and mercaptophenylboronic acid (PBA) could bind to cis-diol moieties in the ADP-ribose units to form borate ester compounds (Fig. 4) [8]. Once PARP-1 was captured by the dsDNA-modified magnetic beads (MBs), auto-PARylation was initiated and the PAR polymers consisting of abundant ribose units were covalently bound to FcBA or MPBA molecules. The sequestration of FcBA or MPBA by the PAR-covered MBs resulted in the decrease of electrochemical signal or the prevention of MPA-triggered AuNPs aggregation. The oxidation current and adsorption intensity are related to the concentration and activity of PARP-1. The linear range of both electrochemical and colorimetric method was found to be 0.1 ~ 50 U.

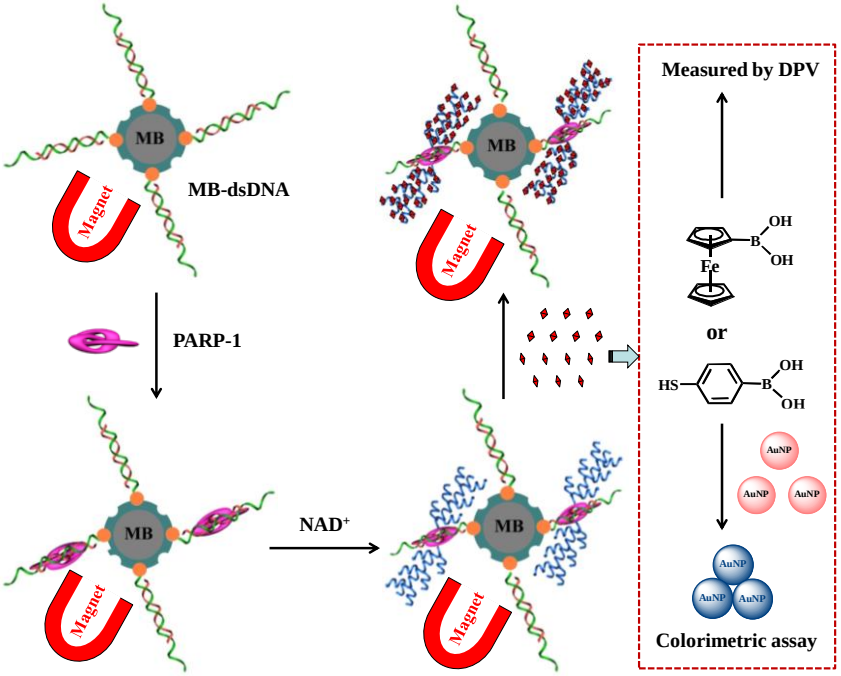

Figure 4. Schematic illustration of magnetic-based electrochemical and colorimetric strategies for PARP-1 detection by sequestrating FcBA or MPBA. Reprinted with permission from reference [8]. Copyright 2021 Elsevier.

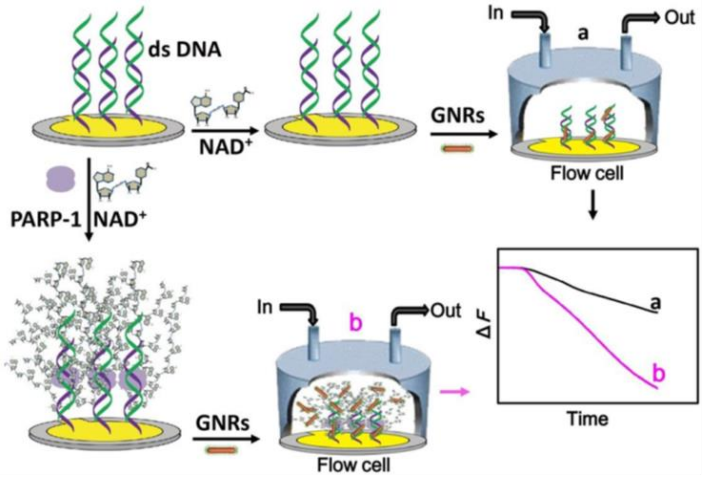

Figure 5. Schematic representation of the sensing process of amplified QCM biosensor based on GNRs. Reprinted with permission from reference [20]. Copyright 2019 American Chemical Society.

Moreover, Yang et al. developed a quartz microbalance method to determine PARP-1 activity by the signal amplification of gold nanorods (GNRs) [20]. As shown in Fig. 5, PARP-1 was activated by the dsDNA to hydrolyze NAD^+ and form the hyperbranched PAR polymers. Although quartz microbalance is sensitive to mass, it is still not enough to detect PAR polymer effectively. However, the sensitivity has been improved by the binding of GNRs. The linear range of this method is 0.06 ~ 3 nM, and the detection limit is 0.04 nM.

As an alternate electrochemical technology, photoelectrochemical (PEC) biosensors, integrating the merits of biological and optical assays, have been widely concerned in the field of biosensing [36]. The background signal of PEC biosensors is low due to the separation of excitation source and detection signal. For this consideration, Liu's group developed the first PEC biosensor for PARP-1 detection [30]. In this work, the positively charged poly[9,9-bis(6'-N,N,N-trimethylammonium)hexyl]fluorenylene phenylene (PFP) with good PEC property was captured by the PAR polymer through the electrostatic interaction. The photocurrent changed linearly with the increase of PARP-1 concentration in the range of 0.01 ~ 2 U. The detection limit was found to be 0.007 U.

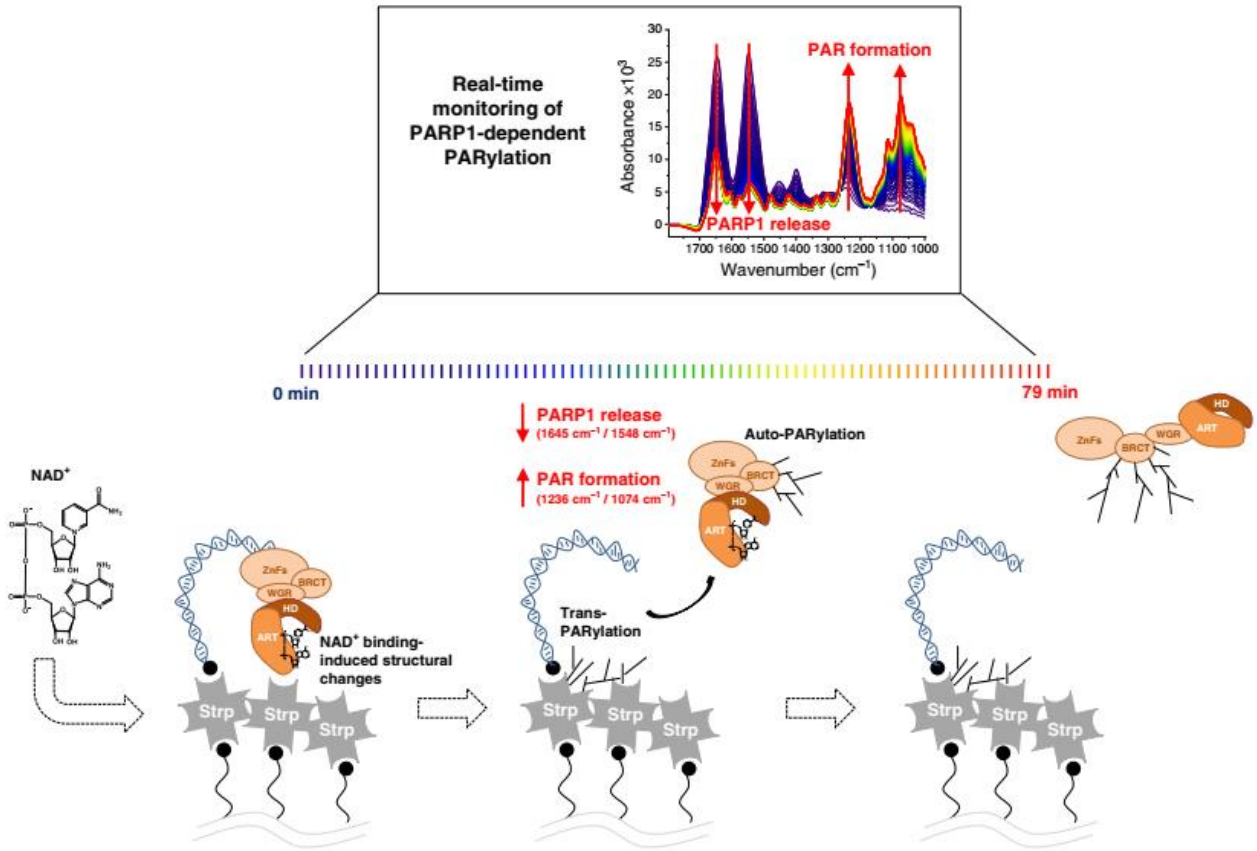

Figure 6. Mechanistic model of PARP1-dependent PARylation derived by time-resolved ATR-FTIR spectroscopy. Reprinted with permission from reference [11]. Copyright 2020 Nature.

4. CONCLUSION

In summary, the work summarized the electrochemical methods for PARP-1 detection. After binding to the DNA probe on the electrode surface, PARP-1 can be activated to generate the PAR polymers in PARP-1 itself. Based on the electrostatic interaction or the boronate ester covalent bond, the resulting PAR polymers can be monitored by different electrochemical techniques. The developed methods are sensitive and interesting. However, the dissociation and inactivation of PARP1 after PARylation should be investigated for the design and application of novel PARP-1 biosensors since the dissociation of auto-modified PARP1 from DNA was monitored by ATR-FTIR spectroscopy (Fig.

6). Moreover, electrochemical technique may provide a platform to monitor the enzymatic process and reveal the mechanism of PARP1-dependent PARylation.

ACKOWLEDGMENTS
This work was supported by the Guizhou Education University Doctor Program (2019BS008) and (2019BS009), Guizhou University integrated research platform (QJHKY(2020)008), and the Natural Science Foundation of Department of Education of Guizhou Province ([2021]021).

References

1. Y. Wang, R. An, G.K. Umanah, H. Park, K. Nambiar, S.M. Eacker, B.W. Kim, L. Bao, M.M. Harraz, C. Chang, R. Chen, J.E. Wang, T.-I. Kam, J.S. Jeong, Z. Xie, S. Neifert, J. Qian, S.A. Andrabi, S. Blackshaw, H. Zhu, H. Song, G.-L. Ming, V.L. Dawson and T.M. Dawson, *Science*, 354 (2016) 6872-6813.
2. M.-F. Langelier, J.L. Planck, S. Roy and J.M. Pascal, *Science*, 336 (2012) 728.
3. Y. Wang, V. Dawson and T. Dawson, *Exp. Neurol.*, 218 (2009) 193.
4. S.-W. Yu, H. Wang, M.F. Poitras, C. Coombs, W.J. Bowers, H.J. Federoff, G.G. Poirier, T.M. Dawson and V.L. Dawson, *Science*, 297 (2002) 259.
5. C. Powell, C. Mikropoulos, S.B. Kaye, C.M. Nutting, S.A. Bhide, K. Newbold and K.J. Harrington, *Cancer Treat Rev*, 36 (2010) 566.
6. F. Rojo, J. Garcia-Parra, S. Zazo, I. Tusquets, J. Ferrer-Lozano, S. Menendez, P. Eroles, C. Chamizo, S. Servitja and N. Ramirez-Merino, *Ann. Oncol.* , 23 (2011) 1156.
7. S. Pazzaglia and C. Pioli, *Cells*, 9 (2019) 41.
8. N. Xia, D. Wu, T. Sun, Y. Wang, X. Ren, F. Zhao, L. Liu and X. Yi, *Sens. Actuat. B: Chem.*, 327 (2021) 128913.
9. P. Decker, E.A. Miranda, G. de Murcia and S. Muller, *Clin. Cancer Res.*, 5 (1999) 1169.
10. E. Bakondi, P. Bai, E. Szabó E, J. Hunyadi, P. Gergely, C. Szabó and L. Virág, *J. Histochem. Cytochem.*, 50 (2002) 91.
11. A. Krüger, A. Bürkle, K. Hauser and A. Mangerich, *Nat. Commun.*, 11 (2020) 2174.
12. E. Xu, H. Yang, P. Li, Z. Wang, Y. Liu, W. Wei and S. Liu, *Sens. Actuat. B: Chem.*, 330 (2021) 129288.
13. S. Wu, C. Chen, H. Yang, W. Wei, M. Wei, Y. Zhang and S. Liu, *Sens. Actuat. B: Chem.*, 273 (2018) 1047.
14. H. Yang, F. Fu, W. Li, W. Wei, Y. Zhang and S. Liu, *Chem. Sci.*, 10 (2019) 3706.
15. Y. Liu, X. Xu, H. Yang, E. Xu, S. Wu, W. Wei and J. Chen, *Analyst*, 143 (2018) 2501.
16. Y. Liu, E. Xu, C. Xu and W. Wei, *Sens. Actuat. B: Chem.*, 325 (2020) 128806.
17. S. Wu, M. Wei, H. Yang, J. Fan, W. Wei, Y. Zhang and S. Liu, *Sens. Actuat. B: Chem.*, 259 (2018) 565.
18. Y. Xu, J. Wang, Y. Cao and G. Li, *Analyst*, 136 (2011) 2044.
19. D. Zhang, K. Wang, W. Wei and S. Liu, *ACS Sens.*, 5 (2020) 1198.
20. H. Yang, P. Li, D. Wang, Y. Liu, W. Wei, Y. Zhang and S. Liu, *Anal. Chem.*, 91 (2019) 11038.
21. S. Tang, Z. Nie, W. Li, D. Li, Y. Huang and S. Yao, *Chem. Commun.*, 51 (2015) 14389.
22. Y. Liu, J. Fan, H. Yang, E. Xu, W. Wei, Y. Zhang and S. Liu, *Biosens. Bioelectron.*, 113 (2018) 136.
23. R.R. Rustandi, M. Hamm, J.W. Loughney and S. Ha, *Electrophoresis*, 36 (2015) 2798.
24. X. Ma, *Int. J. Electrochem. Sci.*, 15 (2020) 7663.
25. Y. Xu, L. Liu, Z. Wang and Z. Dai, *ACS Appl. Mater. Interfaces*, 8 (2016) 18669.

26. E. Xu, H. Yang, L. Wu, J. Chen, W. Wei, Y. Liu and S. Liu, *Sens. Actuat. B: Chem.*, 294 (2019) 185.
27. Y. Liu, J. Fan, L. Shangguan, Y. Liu, Y. Wei, W. Wei and S. Liu, *Talanta*, 180 (2018) 127.
28. X. Zhou, C. Wang, Z. Wang, H. Yang, W. Wei, Y. Liu and S. Liu, *Biosens. Bioelectron.*, 148 (2020) 111810.
29. Z. Wang, E. Xu, C. Wang, W. Wei, Y. Liu and S. Liu, *Anal. Chim. Acta*, 1091 (2019) 95.
30. C. Wang, Y. Li, E. Xu, Q. Zhou, J. Chen, W. Wei, Y. Liu and S. Liu, *Biosens. Bioelectron.*, 138 (2019) 111308.
31. N. Xia, D. Wu, H. Yu, W. Sun, X. Yi and L. Liu, *Talanta*, 221 (2021) 121640.
32. L. Liu, N. Xia, Y. Xing and D. Deng, *Int. J. Electrochem. Sci.*, 8 (2013) 11161.
33. L. Liu, C. Cheng, Y. Chang, H. Ma and Y. Hao, *Sens. Actuat. B: Chem.*, 248 (2017) 178.
34. L. Hou, Y. Huang, W. Hou, Y. Yan, J. Liu and N. Xia, *Int. J. Biol. Macromol.*, 158 (2020) 580.
35. N. Xia, L. Liu, Y. Chang, Y. Hao and X. Wang, *Electrochem. Commun.*, 74 (2017) 28.
36. L. Hou, B. Zhou, Y. Li and M. La, *Int. J. Electrochem. Sci.*, 14 (2019) 4453